

Studies with Guanidinium- and Amidinium-Based Inhibitors Suggest Minimal Stabilization of Allylic Carbocation Intermediates by Dehydrosqualene and Squalene Synthases

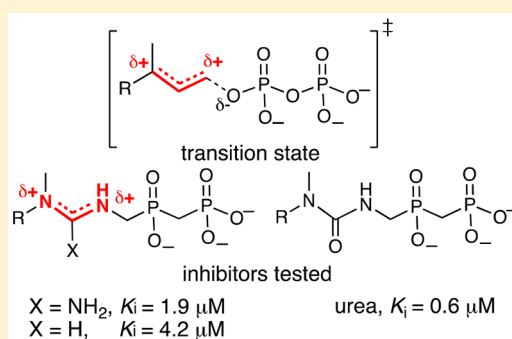
Walid M. Abdelmagid,[†] Taniya Adak,[†] Jon O. Freeman,[‡] and Martin E. Tanner^{*,†}

[†]Department of Chemistry, University of British Columbia, Vancouver, British Columbia V6T 1Z1, Canada

[‡]Department of Chemistry, Pacific Lutheran University, Tacoma, Washington 98447, United States

Supporting Information

ABSTRACT: Dehydrosqualene and squalene synthases catalyze the redox neutral and the reductive, head-to-head dimerization of farnesyl diphosphate, respectively. In each case, the reaction is thought to proceed via an initial dissociation of farnesyl diphosphate to form an allylic carbocation-pyrophosphate ion pair. This work describes the synthesis and testing of inhibitors in which a guanidinium or amidinium moiety is flanked by a phosphonylphosphinate group and a hydrocarbon tail. These functional groups bear a planar, delocalized, positive charge and therefore should act as excellent mimics of an allylic carbocation. An inhibitor bearing a neutral urea moiety was also prepared as a control. The positively charged inhibitors acted as competitive inhibitors against *Staphylococcus aureus* dehydrosqualene synthase with K_i values in the low micromolar range. Surprisingly, the neutral urea inhibitor was the most potent of the three. Similar trends were seen with the first half reaction of human squalene synthase. One interpretation of these results is that the active sites of these enzymes do not directly stabilize the allylic carbocation via electrostatic or π -cation interactions. Instead, it is likely that the enzymes use tight binding to the pyrophosphate and lipid moieties to promote catalysis and that electrostatic stabilization of the carbocation is provided by the bound pyrophosphate product. An alternate possibility is that these inhibitors cannot bind to the “ionization FPP-binding site” of the enzyme and only bind to the “nonionizing FPP-binding site”. In either case, all reported attempts to generate potent inhibitors with cationic FPP analogues have been unsuccessful to date.



Prenyltransferases, prenyldiphosphate synthases, and terpene synthases are all enzymes that utilize allylic diphosphates during catalysis.^{1–3} These enzymes play key roles in a variety of biological processes, and their inhibitors have potential applications in treating cancer, lowering cholesterol, and acting as antimicrobials.^{4,5} In each case, the reaction is initiated by the cleavage of the allylic diphosphate C–O bond, either in a dissociative sense (S_N1) to form an allylic carbocation-pyrophosphate ion pair^{6–9} or in an associative sense (S_N2) via a transition state bearing a considerable carbocationic character.^{10–12} In this work, inhibitors bearing either a guanidinium or an amidinium moiety as a mimic of the allylic carbocation are described (Figure 1). These functional groups are planar, bear a delocalized positive charge at physiological pH values, and should therefore closely resemble the intermediates and/or transition states formed in these reactions.^{3,5,13–16} They are appended to a phosphonylphosphinate group, which acts as a nonhydrolyzable pyrophosphate analogue. In theory, this inhibition strategy could be applied to all three classes of enzymes mentioned above.

In this work, this inhibition strategy is tested on the human squalene synthase (SQS) and the bacterial dehydrosqualene

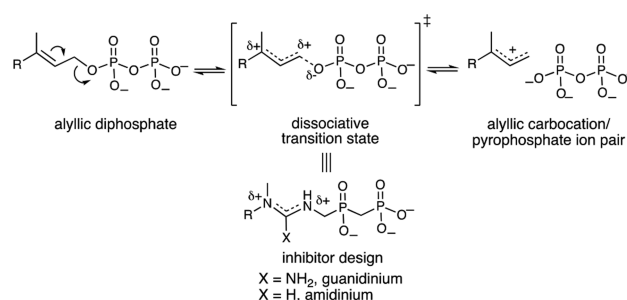


Figure 1. Formation of an allylic carbocation-pyrophosphate ion pair via a dissociative mechanism and the structure of guanidinium/amidinium-based inhibitors designed to mimic the transition state.

synthase (DSQS) from *Staphylococcus aureus*. These enzymes both catalyze the head-to-head condensation of two molecules of farnesyl diphosphate (FPP, Figure 2). Squalene synthase catalyzes a reductive condensation that employs NADPH and

Received: July 6, 2018

Revised: August 24, 2018

Published: September 4, 2018

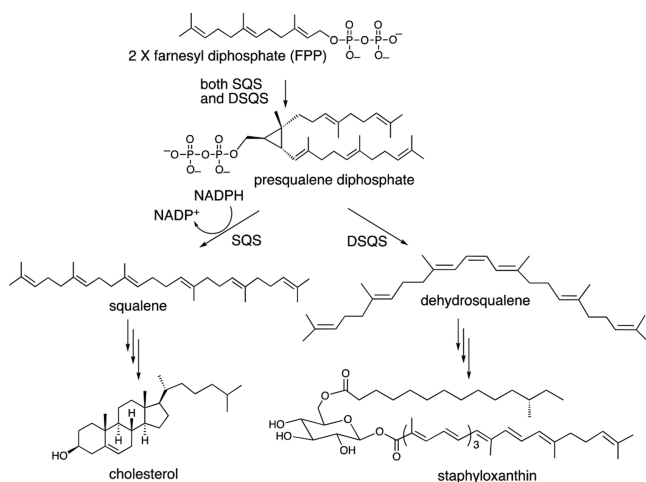


Figure 2. Reactions catalyzed by squalene synthase (SQS) and dehydroqualene synthase (DSQS) and the structures of cholesterol and staphyloxanthin.

generates squalene with a saturated central C–C bond.¹⁷ Alternatively, dehydroqualene synthase catalyzes a redox neutral reaction and generates dehydroqualene with a central alkene.¹⁸ Both enzymes are thought to initiate catalysis by the ionization of FPP to give an allylic cation-pyrophosphate ion pair.^{18,19} A subsequent addition of a second molecule of FPP and deprotonation gives the common intermediate presqualene diphosphate. Presqualene diphosphate is ultimately converted to squalene by SQS or dehydroqualene by DSQS in either a reductive or redox neutral process, respectively.^{20,21} While the overall amino acid sequence similarity between the two enzymes is low (<10%), they share a class I terpenoid synthase fold as well as three conserved consensus sequences that are known to comprise the FPP-binding sites.^{19,22,23} In the case of squalene synthase, the rate limiting step has been shown to occur during presqualene diphosphate formation and a reasonable candidate is the initial ionization step.²⁴ This implies that the dissociation of the FPP C–O bond is a reasonable target for inhibitor design.

Human squalene synthase has long been a target for inhibitor design due to its role in the biosynthesis of steroids.^{13,25} In particular, cholesterol is biosynthesized from squalene, and therefore, compounds that disrupt this pathway could act as cholesterol lowering agents (Figure 2). This strategy could have an advantage over the more commonly used statin drugs that target an earlier step of the mevalonate pathway and therefore stop the production of terpenes entirely. Potent squalene synthase inhibitors include the zaragozic acids and lapaquistat, the latter of which reached late stage development as a cholesterol lowering agent, but trials were ultimately stopped due to liver toxicity.^{26,27}

Dehydroqualene synthase from *S. aureus* has also been suggested as a target for antibiotic development.^{18,28} In this species of bacteria, dehydroqualene is ultimately converted into the polyunsaturated chromophore of the compound staphyloxanthin (Figure 2). Staphyloxanthin is a carotenoid pigment that gives these bacteria their characteristic yellow color. It serves as an antioxidant, which protects the bacteria against reactive oxygen species and host neutrophils.²⁹ It has been demonstrated that treatment of *S. aureus* with DSQS inhibitors results in colorless bacteria that exhibit an increased

sensitivity to the presence of human blood and an increased rate of innate immune clearance in a mouse infection model.²⁸

To test this inhibition strategy against SQS and DSQS, three potential inhibitors were prepared. Inhibitors 1 and 2 are mimics of farnesyl diphosphate bearing a guanidinium and an amidinium moiety, respectively (Figure 3). Inhibitor 3 is an

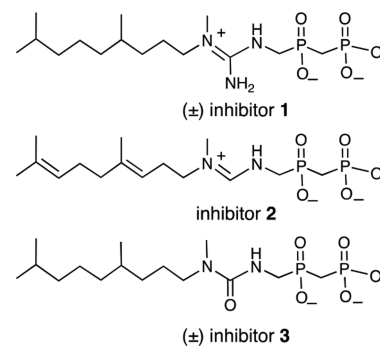


Figure 3. Structures of inhibitors 1–3.

isosteric analogue of inhibitor 1 that bears a urea linkage and serves as a control to test whether the charged guanidinium group contributes significantly to inhibition. It is shown that these compounds act as competitive inhibitors in the low micromolar range and that the delocalized positive charge does not contribute significantly to binding affinity. These results suggest that direct stabilization of the allylic carbocation intermediate is not a key factor in catalysis with these enzymes.

■ MATERIALS AND METHODS

Synthetic Materials and Methods. All reagents were purchased from Sigma-Aldrich, Fluka, Toronto Research Chemicals Inc. (TRC), or Advanced ChemTech and used without further purification unless otherwise stated. D₂O (99.9%) was purchased from Cambridge Laboratories. Dowex 50WX8 (H⁺ form) resin was purchased from Sigma-Aldrich. Triethylamine was distilled over CaH₂ under an atmosphere of Ar. Silica gel chromatography was performed using Silica Gel SiliaFlash F60 (230–400 mesh, Silicycle). Biogel P-2 size exclusion chromatography resin was purchased from Bio-Rad. ¹H NMR spectra were recorded on a Bruker AV400 spectrometer at a field strength of 400 MHz. Proton-decoupled ³¹P NMR spectra were recorded on a Bruker AV400 spectrometer at a field strength of 162 MHz. ¹³C NMR spectra were recorded on a Bruker AV400 spectrometer at a field strength of 100 MHz. Mass spectra were obtained on a Waters Micromass LCT mass spectrometer using electrospray ionization (ESI-MS). Neutral compounds were detected as positive ions, and negatively charged compounds were detected as negative ions.

Enzymology Materials and Methods. Centrifugal filters (4 mL 10 000 MWCO) were purchased from Millipore. Isopropyl-β-D-galactopyranoside (IPTG) was purchased from Invitrogen. Chelating Sepharose Fast resin was purchased from Pharmacia Biotech. Protein concentrations were determined by the method of Bradford on a Cary 3E UV–vis spectrophotometer using bovine serum albumin as a standard.³⁰ These measurements were performed at room temperature. Protein purity was assessed using SDS-PAGE. The enzyme kinetic assays were carried out on a Cary 300 UV–vis spectrometer with a Cary temperature controller attached.

Overexpression and Purification of HSQS and DSQS.

The gene encoding for dehydrosqualene synthase from *S. aureus* MS4 was synthesized and cloned into a pET28a(+) vector at the BamHI and Sall restriction sites by Genscript. A stop codon was added after the DSQS open reading frame to prevent expression of pET28a's optional C-terminal His tag. Expression of the resulting plasmid, pETa-DSQS, results in a protein expressed with an N-terminal His tag and T7 tag. The codon optimized gene for doubly truncated human squalene synthase (residues 31–370) was synthesized by GenScript and cloned into a pET28b expression vector (Novagen) via the NdeI/XhoI restriction sites, yielding pET28b-hSQS(31–370). A stop codon was added after the SQS open reading frame to prevent expression of pET28b's optional C-terminal His tag. The resulting construct encoded hSQS(31–370) with an N-terminal His tag followed by a thrombin protease recognition site. Both plasmids were used to transform chemically competent *Escherichia coli* expression strain Rosetta(DE3) pLysS (Novagen) following the Inoue method.³¹ Overproduction of DSQS and SQS was achieved following a modification of a previously described procedure.³² Transformed cells were grown at 37 °C in 1 L of Terrific Broth (TB) medium containing 30 µg/mL kanamycin until an OD₆₀₀ of 0.6 was reached. Cells were induced for overexpression by the addition of 120 mg (1 mM) of isopropyl-1-thio-β-D-galactopyranoside (IPTG). After growing at 24 °C for an additional 24 h, cells were harvested and lysed with a French press in Tris-HCl buffer (50 mM, pH 8.0) containing dithiothreitol (2 mM), NaCl (500 mM), MgCl₂ (2 mM), CHAPS (4 mM), imidazole (20 mM), aprotinin (1 µg mL⁻¹), and pepstatin A (1 µg mL⁻¹).

The lysate was cleared by centrifugation (34 155g, 45 min) and filtration through a 0.22 µm filter. A column containing chelating Sepharose fast flow resin (GE Healthcare, 10 mL) was charged with 100 mM NiSO₄ and washed with Tris-HCl buffer (50 mM, pH 8.0) containing NaCl (500 mM) and imidazole (5 mM). The clarified lysate was loaded onto the column and eluted with same buffer but containing imidazole at 5, 20, 100, and 500 mM. Fractions containing the desired enzyme eluted after the addition of 500 mM imidazole as analyzed by the Bradford assay. Glycerol (10%) was added to the resulting eluent before flash freezing with liquid N₂. Typically, 20–30 mg of enzyme was purified from 1 L of culture. Enzymes were found to be more than 90% pure as analyzed by SDS-PAGE. The enzymes were used without the removal of the hexahistidine tags.

Measurement of Enzyme Kinetics. Kinetic parameters of dehydrosqualene synthase (DSQS) were measured by a modification of a previously described continuous coupled assay for phosphate release.^{8,33} The concentrations of stock solutions of the inhibitors in D₂O, containing an internal standard of dioxane, were determined by ¹H NMR integration. A cuvette containing 50 mM HEPES buffer (pH 7.50, final volume 1000 µL, containing 5% EtOH), MgCl₂ (5 mM), farnesyl pyrophosphate (50 µM, added from a stock solution prepared in 40% EtOH), 2-amino-6-mercapto-7-methylpurine ribonucleoside (MESG) (20 µM), purine nucleoside phosphorylase (PNPase) (1 unit), and inorganic pyrophosphatase (PPase) (0.5 unit) was thermally equilibrated for 5 min at 37 °C. The enzymatic reaction was initiated by the addition of dehydrosqualene synthase (1.5 µg), and the rate was calculated from the observed increase of absorption at 360 nm ($\epsilon = 11\,000\text{ M}^{-1}\text{ cm}^{-1}$) after accounting for the 4:1 ratio of

phosphate to dehydrosqualene. Kinetic parameters were determined from the fit of initial velocities to the Michaelis–Menten equation. SQS kinetics were determined in the same fashion; however, 2.0 µg of enzyme was added, and the 2:1 ratio of phosphate to squalene was accounted for. Inhibition kinetics were described as above, but with the incubation of inhibitors 1–3 at various concentrations.

Synthetic Methods. Compound 5. A solution of 4 (1.23 g, 7.53 mmol) in dry Et₂O was added dropwise to a suspension of lithium aluminum hydride (0.343 g, 9.04 mmol) in 35 mL of dry Et₂O at 0 °C. The reaction mixture was refluxed at 35 °C for 15 h under Ar. It was quenched by successive addition of 0.4 mL of H₂O, 0.8 mL of 10% aq NaOH, and another 1.2 mL of H₂O. After the resulting mixture was stirred for 15 min, it was filtered through a Celite bed and the clear solution was dried over MgSO₄. The solution was dried in a vacuum to afford compound 5 (1.26 g, 99% yield). ¹H NMR (CDCl₃, 400 MHz): δ ppm 5.09 (m, 2H), 2.72 (t, $J = 6.8$ Hz, 2H), 2.19–2.17 (m, 2H), 2.09–2.06 (m, 2H), 2.03–1.99 (m, 2H), 1.68 (s, 3H), 1.63 (s, 3H), 1.60 (s, 3H). HRMS (ESI) m/z : $[M + H]^+$ calcd for C₁₁H₂₁N, 168.1752; found, 168.1744.

Compound 6. Compound 5 (0.699 g, 4.18 mmol) was dissolved in ethylformate (3.80 mL, 46.6 mmol), and the mixture was refluxed for 18 h at 55 °C under Ar. The volatile components were removed in a vacuum, and the resulting oily residue was purified using silica gel column chromatography (3:5 EtOAc/petroleum ether) to afford compound 6 (0.60 g, 79%). ¹H NMR (CDCl₃, 400 MHz) 4:1 mixture of rotamers: δ ppm {8.14 (major, s), 8.04 (minor, d, $J = 12.1$ Hz)} (1H), 5.53 (br s, 1H), 5.08 (m, 2H), {3.32 (major), 3.23 (minor)} (td, $J = 6.8$ Hz, 0.9 Hz, 2H), 2.26–2.21 (m, 2H), 2.09–2.06 (m, 2H), 2.04–2.02 (m, 2H), 1.68 (s, 3H), 1.62 (s, 3H), 1.60 (s, 3H). ESI-MS m/z : 218.3 $[M + Na]^+$.

Compound 7. A solution of 6 (2.45 g, 12.5 mmol) in dry Et₂O was added dropwise to a suspension of lithium aluminum hydride (0.953 g, 25.1 mmol) in 35 mL of dry Et₂O at 0 °C. The reaction mixture was warmed to 35 °C and refluxed for 15 h under Ar. It was quenched by successive addition of 1 mL of H₂O, 2 mL of 10% aq NaOH, and another 3 mL of H₂O. After the resulting mixture was stirred for 15 min, it was filtered through a Celite bed and the clear solution was dried over MgSO₄. The solution was dried in a vacuum to afford 7 (2.15 g, 95%). ¹H NMR (CDCl₃, 400 MHz): δ ppm 5.08 (m, 2H), 2.58 (t, $J = 6.9$ Hz, 2H), 2.43 (s, 3H), 2.20 (q, $J = 7.1$ Hz, 2H), 2.11–1.93 (m, 4H), 1.68–1.57 (m, 9H). HRMS (ESI) m/z : $[M + H]^+$ calcd for C₁₂H₂₃N, 182.1830; found, 182.1829.

Compound ±8. Compound 7 (2 g, 11 mmol) was dissolved in EtOH (50 mL), and 10% Pd/C catalyst (200 mg) was added. The mixture was stirred under 1 atm of H₂ (g) for 18 h at rt. The catalyst was removed by filtration, and the resulting filtrate was evaporated to dryness under reduced pressure. This gave compound 8 as a viscous oil (1.8 g, 99%). ¹H NMR (CDCl₃, 400 MHz): δ ppm 2.56 (t, $J = 6.2$, 2H), 2.48 (s, 3H), 1.58–0.85 (m, 12H), 0.79 (d, $J = 6.6$ Hz, 9H). ESI-MS m/z : 186.4 $[M + H]^+$.

Compound 10. *N,N*-Di-Boc-thiourea (410 mg, 1.53 mmol) and NaH (80 mg, 2.1 mmol) were stirred in dry THF (20 mL) under argon for 25 min at 0 °C. Trifluoroacetic anhydride (300 µL, 1.75 mmol) was then added, and the mixture was left stirring for 1 h at 0 °C, followed by the addition of compound 9 (400 mg, 1.75 mmol). The reaction mixture was stirred at rt for 20 h and quenched with H₂O, and the product was extracted with CH₂Cl₂ (3 × 50 mL). The organic layers were

dried over MgSO_4 and then concentrated under reduced pressure to yield a yellow oil. The crude product was purified using column chromatography (15–100% EtOAc in petroleum ether) to afford compound **10** (400 mg, 60%). ^1H NMR (CDCl_3 , 400 MHz): δ ppm 10.09 (s, 1H), 8.09 (s, 1H), 4.47 (m, 2H), 4.34–4.05 (m, 6H), 2.54 (t, $J = 17.3$ Hz, 2H), 1.47 (s, 9H), 1.24 (t, $J = 7.1$ Hz, 6H), 1.19 (t, $J = 5.1$ Hz, 3H). $^{31}\text{P}\{^1\text{H}\}$ NMR (CDCl_3 , 162 MHz): δ ppm 19.72 (s), 40.05 (s). ESI-MS m/z : 433.1 $[\text{M} + \text{H}]^+$.

Compound 12. Compound **10** (180 mg, 0.41 mmol), DIPEA (80 μL , 0.41 mmol), EDC-HCl (170 mg, 0.83 mmol), and compound ± 8 (120 mg, 0.62 mmol) were dissolved in dry CH_2Cl_2 (15 mL) at 0 °C, and the mixture was stirred under argon for 25 h at rt. The reaction mixture was then quenched with H_2O and then extracted with CH_2Cl_2 (3×50 mL). The organic layers were dried over MgSO_4 and concentrated under reduced pressure to yield an oil. The crude product was purified using column chromatography (1–15% MeOH in EtOAc containing 5% Et_3N) to afford compound **12** (140 mg, 60%). ^1H NMR (CDCl_3 , 400 MHz): δ ppm 4.24–4.05 (m, 6H), 3.72 (m, 2H), 3.25 (m, 2H), 2.95 (s, 3H), 2.62–2.43 (m, 2H), 2.07–1.95 (m, 2H), 1.68–1.48 (m, 10H), 1.45 (s, 9H), 1.32 (m, 9H), 1.25 (m, 6H), 1.13 (t, $J = 5.7$ Hz, 3H). $^{31}\text{P}\{^1\text{H}\}$ NMR (CDCl_3 , 162 MHz): δ ppm 20.05 (s), 44.50 (s). HRMS (ESI) m/z : $[\text{M} + \text{H}]^+$ calcd for $\text{C}_{21}\text{H}_{47}\text{N}_3\text{O}_5\text{P}_2$, 586.5711; found, 586.5701.

Inhibitor 1. Compound **12** (100 mg, 0.17 mmol) was treated with TMSBr (1 mL) in CH_2Cl_2 (10 mL), and the mixture was stirred at rt for 18 h. The solution was then neutralized with NaOH (0.1 M) and concentrated under reduced pressure to yield a yellow oil. The compound was then dissolved in H_2O (10 mL) and acidified with Dowex resin (H^+ form) to pH 1. The crude material was then dissolved in H_2O (10 mL), loaded onto a 50 mL column of size exclusion resin (Bio-Gel P-2), and eluted with water. All fractions were lyophilized to dryness and analyzed using ^1H and ^{31}P NMR spectroscopy. Fractions containing the inhibitor were redissolved in water, combined, and lyophilized to give inhibitor **1** as a white solid (18 mg, 25%). ^1H NMR (MeOD, 400 MHz): δ ppm 3.55 (d, $J = 8.6$ Hz, 2H), 3.31–3.28 (m, 2H), 3.03 (s, 3H), 2.25–2.04 (m, 2H), 1.72–1.02 (m, 12H), 0.86 (d, $J = 5.5$ Hz, 9H). $^{31}\text{P}\{^1\text{H}\}$ NMR (MeOD, 162 MHz): δ ppm 18.66 (s), 33.04 (s). HRMS (ESI) m/z : $[\text{M} + \text{H}]^+$ calcd for $\text{C}_{15}\text{H}_{35}\text{N}_3\text{O}_5\text{P}_2$, 400.2101; found, 400.2133.

Compound 13. A solution of the amine **9** (437 mg, 1.59 mmol) and *N,N*-dimethylformamide dimethyl acetal (0.64 mL, 4.80 mmol) in 5 mL of distilled methanol was heated to 55 °C under Ar for 4.5 h. All volatile components were removed under reduced pressure to obtain compound **13** as an oily residue (513 mg, 98%). The compound was characterized without further purification. ^1H NMR (CDCl_3 , 400 MHz): δ ppm 7.38 (s, 1H), 4.27–4.07 (m, 6H), 3.85–3.68 (m, 2H), 2.88 (s, 6H), 2.52 (dd, $J = 20.6$, 16.2 Hz, 2H), 1.41–1.28 (m, 9H). $^{31}\text{P}\{^1\text{H}\}$ NMR (CDCl_3 , 162 MHz): δ ppm 43.79 (d, $J = 5.9$ Hz), 20.62 (d, $J = 6.1$ Hz). ESI-MS m/z : 351.2 $[\text{M} + \text{Na}]^+$.

Compound 14. To a stirred solution of compound **13** (89.4 mg, 0.272 mmol) in distilled acetonitrile under Ar was added compound **7** (115 mg, 0.634 mmol). The reaction mixture was secured with a reflux condenser and was heated to 75 °C. The reaction mixture was cooled down after 48 h and was concentrated under a high vacuum. The yellowish oily residue was purified using silica gel (equilibrated with 5% Et_3N in the

eluent system) column chromatography (1:10 MeOH/EtOAc containing 2% Et_3N). Volatilizing the solvents gave the desired compound **14** (24.2 mg, 38%). ^1H NMR (CDCl_3 , 400 MHz): δ ppm 7.38 (s, 1H), 5.06 (m, 2H), 4.21–4.16 (m, 6H), 3.76 (dd, $J = 11.7$, 4.1 Hz, 2H), 3.15 (s, 2H), 2.87 (s, 3H), 2.50 (dd, $J = 20.6$, 16.2 Hz, 2H), 2.20 (td, $J = 7.2$ Hz, 0.2 Hz, 2H), 2.07–1.95 (m, 4H), 1.67 (s, 3H), 1.59 (s, 6H), 1.35–1.31 (m, 9H). $^{31}\text{P}\{^1\text{H}\}$ NMR (CDCl_3 , 162 MHz): δ ppm 43.68 (s), 20.70 (d, $J = 5.7$ Hz). HRMS (ESI) m/z : $[\text{M} + \text{H}]^+$ calcd for $\text{C}_{21}\text{H}_{42}\text{N}_2\text{O}_5\text{P}_2$, 465.2647; found, 465.2649.

Inhibitor 2. Compound **14** (25.1 mg, 0.054 mmol) was dissolved in 3 mL of distilled CH_2Cl_2 in a flame-dried round-bottom flask, and the mixture was cooled to 0 °C. Dried 2,4,6-collidine (121 μL , 0.915 mmol) was slowly added to the reaction mixture followed by the addition of TMSBr (149 μL , 1.13 mmol). The reaction mixture was stirred at rt for 24 h or until ESI-MS analysis confirmed the completion of the reaction. The volatile materials were removed in a vacuum, and the resulting residue was washed with toluene and concentrated repeatedly to remove any remaining TMSBr. The solid residue was neutralized by the careful addition of an aqueous sodium hydroxide (~2 equiv) solution. Water was evaporated under a high vacuum to give a white solid crude. The desired product eluted with water in two column volumes using size exclusion chromatography (Bio-Gel P-2 Gel). The resulting solution was frozen and lyophilized to give the sodium salt of inhibitor **2** (9 mg, 43%). ^1H NMR (MeOD, 400 MHz), 4:1 mixture of rotamers: δ ppm {6.44 (major), 6.37 (minor)} (s, 1H), 3.62–3.59 (m, 2H), 2.12 (d, $J = 9.3$ Hz, 2H), {1.98 (major), 1.93 (minor)} (t, $J = 7.0$ Hz, 2H), {1.73 (minor), 1.58 (major)} (s, 3H), 0.92–0.88 (m, 2H), 0.74 (t, $J = 18.8$ Hz, 2H), 0.58–0.50 (m, 4H), 0.17 (s, 3H), 0.15 (s, 3H), 0.10 (s, 3H). $^{31}\text{P}\{^1\text{H}\}$ NMR (MeOD, 162 MHz): δ ppm 23.14 (s), 17.41 (s). HRMS (ESI) m/z : $[\text{M} + \text{H}]^+$ calcd for $\text{C}_{15}\text{H}_{30}\text{N}_2\text{O}_5\text{P}_2$, 381.1708; found, 381.1710.

Compound 15. Compound **9** (300 mg, 1.09 mmol) was dissolved in dry CH_2Cl_2 (15 mL), and then Et_3N (275 μL , 1.63 mmol) was added; the mixture was stirred under argon for 30 min. Boc_2O (300 mg, 1.32 mmol) was then added, and the reaction was stirred at rt for 16 h. The reaction mixture was concentrated under reduced pressure, and the crude product was purified using silica gel chromatography (25–75% EtOAc in petroleum ether) to yield pure compound **15** (325 mg, 81%). ^1H NMR (CDCl_3 , 400 MHz): δ ppm 4.30–4.06 (m, 6H), 3.55–3.65 (m, 2H), 2.60–2.36 (m, 2H), 1.49 (s, 9H), 1.45–1.25 (m, 6H), 1.24–1.19 (t, $J = 7.6$ Hz, 3H). $^{31}\text{P}\{^1\text{H}\}$ NMR (CDCl_3 , 162 MHz): δ ppm 20.58 (s), 41.84 (s). ESI-MS m/z : 374.3 $[\text{M} + \text{H}]^+$.

Compound 16. Compound **15** (80 mg, 0.21 mmol) was placed in a round-bottom flask followed by dry CH_2Cl_2 (10 mL). 2-Chloropyridine (60 μL , 0.63 mmol) was added, followed by trifluoromethanesulfonic anhydride (60 μL , 0.31 mmol), and the reaction mixture was stirred for 50 min at rt. Then Et_3N (1.8 mL, 1.26 mmol) followed by the compound ± 8 (116 mg, 0.62 mmol) was added, and the reaction mixture was stirred at rt for 20 h. The crude product was purified using silica gel chromatography (10–50% EtOAc in petroleum ether) to afford compound **16** (66 mg, 65%). ^1H NMR (CDCl_3 , 400 MHz): δ ppm 4.28–4.06 (m, 6H), 3.6–3.72 (m, 2H), 2.95 (m, 2H), 2.76 (s, 3H), 1.85–1.75 (m, 2H), 1.56–1.03 (m, 21H), 0.88–0.94 (m, 9H). $^{31}\text{P}\{^1\text{H}\}$ NMR (CDCl_3 , 162 MHz): δ ppm 22.50 (s), 45 (s). ESI-MS m/z : 483.9 $[\text{M} - \text{H}]^-$.

Inhibitor 3. Compound **16** (100 mg, 0.21 mmol) was treated with TMSBr (1 mL) in CH_2Cl_2 (10 mL), and the mixture was stirred at rt for 18 h. The solution was then neutralized with NaOH (0.1 M) and then was concentrated under reduced pressure to yield a yellow oil. The compound was then dissolved in H_2O (10 mL) and acidified with Dowex resin (H^+ form) to pH 1. The crude material was then dissolved in H_2O (10 mL), loaded onto a 50 mL column of size exclusion resin (Bio-GelP-2), and eluted with water. All fractions were lyophilized to dryness and analyzed using ^1H and ^{31}P NMR spectroscopy. Fractions containing inhibitor were redissolved in water, combined, and lyophilized to give inhibitor **3** as a white solid (48 mg, 56%). ^1H NMR (D_2O , 400 MHz): δ ppm 3.68–3.24 (m, 4H), 2.96 (s, 3H), 2.15–2.09 (m, 2H), 1.73–0.95 (m, 12H), 0.92 (s, 9H). $^{31}\text{P}\{^1\text{H}\}$ NMR (D_2O , 162 MHz): δ ppm 14.79 (s), 36.93 (s). HRMS (ESI) m/z : $[\text{M} + \text{Na}]^+$ calcd for $\text{C}_{15}\text{H}_{34}\text{N}_2\text{O}_6\text{P}_2\text{Na}$, 423.1800; found, 423.1786.

RESULTS

Synthesis of Inhibitors. The lipid portion of all three inhibitors was made from the known nitrile **4**, which is prepared from geraniol in two steps (Figure 4).³⁴ Compound **4**

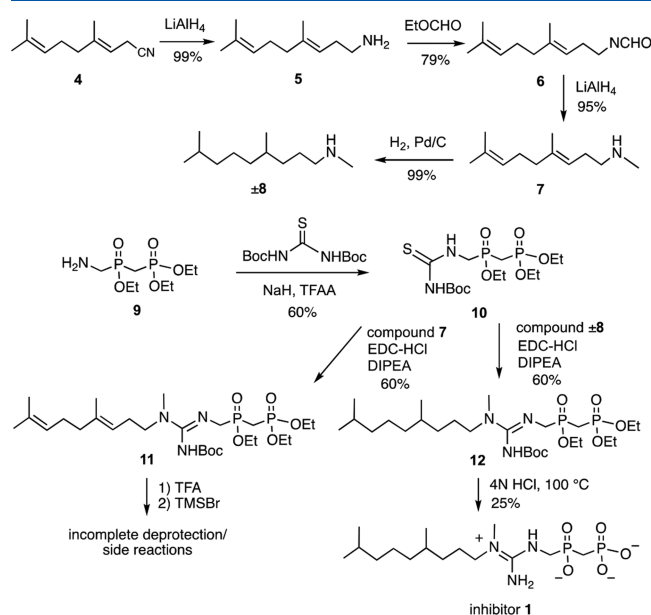


Figure 4. Synthesis of inhibitor **1**.

was reduced to give homogeranylamine **5**, which was then formylated to give compound **6**.³⁵ Reduction of the formyl group gave *N*-methyl-homogeranylamine **7**. In the case of inhibitors **1** and **3**, compound **7** was hydrogenated to give the saturated analogue, racemic **8**.

The phosphonylphosphinate amine **9** was prepared from diethylphosphite, formaldehyde, and diethylmethylphosphonate in seven steps using literature known methods.³⁶ To prepare inhibitor **1**, compound **9** was treated with di-Boc-protected thiourea, trifluoroacetic anhydride, and sodium hydride to give thiourea **10**.³⁷ Thiourea **10** was initially coupled to compound **7** in an attempt to prepare the unsaturated analogue of inhibitor **1**. This was achieved using EDC and provided compound **11**.³⁸ Treatment of compound **11** with TFA removed the Boc-protecting group; however, all

attempts to remove the ethyl groups with TMSBr resulted in either incomplete deprotection or side reactions (primarily hydration) of the alkene functionalities. As it is possible to deprotect the corresponding amidine and urea in the preparation of inhibitors **2** and **3**, respectively (vide infra), the failure of this reaction is likely due to the silylation of the guanidinium NH_2 group, which may cause steric hindrance around the phosphinic acid. The inability to fully deprotect compound **11** prompted the design of inhibitor **1** bearing a fully saturated hydrocarbon tail. Previous studies in the literature have suggested that the alkene functionalities are not key recognition determinants in these enzymes.⁴⁵ Therefore, thiourea **10** was coupled to compound **8** to give compound **12**.³⁸ Compound **12** was fully deprotected by refluxing in 4 N HCl for 48 h. The resulting inhibitor **1** was purified by ion exchange chromatography.

The preparation of inhibitor **2** involved an initial condensation of amine **9** with *N,N*-dimethylformamide dimethyl acetal to give amidine **13** (Figure 5).³⁹ A trans-

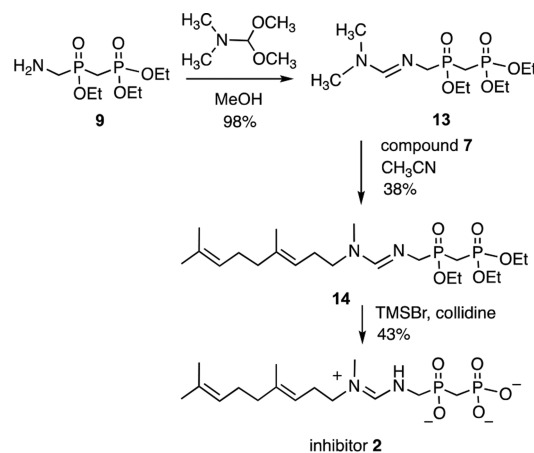


Figure 5. Synthesis of inhibitor **2**.

amidination with *N*-methylhomogeranyl amine **7** liberated dimethylamine and produced amidine **14**.⁴⁰ Care must be taken during the purification of compound **14**, as decomposition to give a formamide occurred during extended exposure to silica gel. Initial attempts to deprotect compound **14** with TMSBr led to side reactions that included hydration of the alkene functionalities. Ultimately, it was possible to deprotect compound **14** using TMSBr in the presence of collidine.^{13,41} This gave inhibitor **2**, which was purified using size exclusion chromatography. In the ^1H NMR spectrum of inhibitor **2**, two rotamers were observed that interconvert slowly on the NMR time scale. These correspond to conformations that differ by the exchange in position of the methyl group and $\text{C}_{11}\text{H}_{19}$ hydrocarbon side chain. Inhibitor **2** was shown to be stable to hydrolysis when stored in a phosphate buffer (pH 7) for 48 h.

For the preparation of inhibitor **3**, compound **9** was first protected with a Boc group to give compound **15** (Figure 6). Compound **15** was treated with triflic anhydride and 2-chloropyridine to produce an intermediate isocyanate that was immediately treated with racemic **8** to give urea **16**.⁴² Deprotection of urea **16** with TMSBr gave racemic inhibitor **3**, which was purified by size exclusion chromatography.³⁶

Enzyme Kinetics. Full-length dehydrosqualene synthase from *S. aureus* and a soluble, truncated, version of human

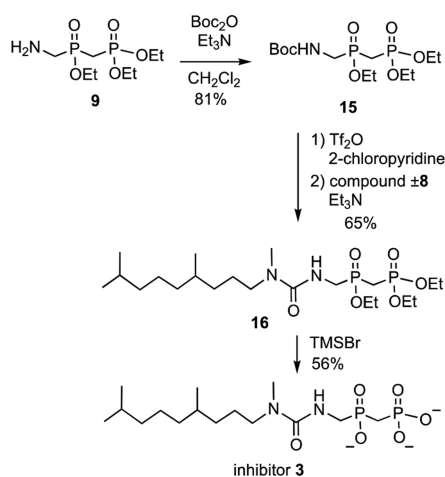


Figure 6. Synthesis of inhibitor 3.

squalene synthase (residues 31–370) were overproduced in *E. coli*.⁴³ Both contained an N-terminal hexa-histidine tag and were purified by immobilized metal affinity chromatography. An assay for phosphate release was used to determine the kinetic parameters.^{8,33} This involves pyrophosphatase as a coupling enzyme that hydrolyzes the pyrophosphate produced in the enzymatic reactions. The resulting phosphate is consumed in a phosphorolysis reaction with 2-amino-6-mercapto-7-methylpurine ribonucleoside and the coupling enzyme, purine nucleoside phosphorylase. The resulting purine product is monitored by an increase in absorbance at 360 nm. The majority of the kinetic analyses were performed with dehydrosqualene synthase as this enzyme does not utilize NADPH in catalysis. In the case of squalene synthase, absorbance from the NADPH chromophore will interfere with the spectrophotometric assay.

The kinetic parameters of dehydrosqualene synthase were first determined using the coupled assay. Varying concentrations of farnesyl diphosphate were incubated with MgCl_2 and dehydrosqualene synthase in a HEPES buffer (pH 7.5) containing 5% ethanol. The reaction was found to follow Michaelis–Menten kinetics and gave the following kinetic parameters: $k_{\text{cat}} = 0.39 \pm 0.01 \text{ s}^{-1}$, $K_{\text{M}} = 25 \pm 5 \mu\text{M}$, and $k_{\text{cat}}/K_{\text{M}} = 16 \times 10^3 \text{ M}^{-1} \text{ s}^{-1}$ (Figure S1). The inhibition by inhibitors 1, 2, and 3 was then evaluated by varying both the inhibitor concentration and the substrate concentration. Lineweaver–Burk plots confirmed that all three acted as competitive inhibitors, and the values of K_{i} were $1.9 \pm 0.08 \mu\text{M}$, $4.2 \pm 0.2 \mu\text{M}$, and $0.61 \pm 0.02 \mu\text{M}$, respectively (Table 1, Figure 7, for Michaelis–Menten plots see Figure S2). It should be noted that DSQS (as well as SQS) has two FPP-binding sites, one in which ionization occurs (the “ionization site”) and one in which the alkene donor binds (the “nonionization

site”), and the K_{M} values measured for FPP could reflect the binding to one, or both, of these sites. Similarly, the inhibitors may bind to one or both of these sites, and the measured K_{i} values could reflect binding to either site. The values of K_{i} were only an order of magnitude lower than that of K_{M} , indicating that either the inhibitors were not significantly benefiting from transition state binding energy or the consequences of replacing a diphosphate functionality with a phosphonylphosphinate offsets these effects. A phosphonylphosphinate would be expected to have increased steric bulk and increased $\text{p}K_{\text{a}}$'s due to the substitution of methylenes for oxygen atoms, and this could perturb metal binding. The similarity in the K_{i} values for compounds 1 and 2 suggest that the presence of the NH_2 moiety of the guanidinium group and the lack of an unsaturated hydrocarbon side chain were not detrimental to binding. Surprisingly, the most potent compound was the urea-containing inhibitor 3. As this inhibitor is effectively isosteric with inhibitor 1, this clearly demonstrates that the inclusion of the positively charged guanidinium as an allylic carbocation mimic does not significantly increase the binding affinity. While resonance delocalization of the nitrogen lone pairs in the urea functionality might be expected to place a partial positive charge on the nitrogen atoms, this is offset by the electronegativity of nitrogen, and the overall charge build-up is expected to be minimal when compared to the full positive charge in an amidinium/guanidinium ion.⁴⁴ This brings into question the extent to which squalene synthase directly stabilizes the allylic cation during catalysis.

Historically, the kinetics of squalene synthase have been measured using a stopped time point radioactive assay with labeled farnesyl diphosphate.^{24,45} This is because the reaction requires the presence of NADPH, and the K_{M} value for this cofactor is $430 \mu\text{M}$ with the human enzyme.⁴⁶ The extremely high absorbance of the NADPH chromophore even at subsaturating levels prohibits the use of a continuous spectrophotometric assay. It is known, however, that squalene synthase binds its substrates in an ordered fashion with two molecules of FPP binding first and NADPH binding last.²⁴ Furthermore, the reaction will proceed in the absence of NADPH to produce presqualene pyrophosphate, followed by a much slower conversion into a mixture of dehydrosqualene and two allylic alcohols.⁴⁷ The formation of presqualene pyrophosphate in the absence of NADPH is much slower than the formation of squalene in the presence of the cofactor, indicating that the presence of NADPH substantially accelerates the first half of the reaction.²⁴ Nevertheless, it is possible to measure the formation of pyrophosphate formed from the first half reaction in the absence of NADPH using the coupled spectrophotometric assay. Given that the inhibitors also bind to a free enzyme (or perhaps a 1:1 FPP–enzyme complex), and therefore compete with the FPP substrates, the inhibition of this “unnatural” process may reflect their affinity for the active site of squalene synthase. The coupled assay was therefore used to analyze the inhibition of the reaction run in the absence of NADPH. Given the caveats above, only IC_{50} values were determined ($[\text{FPP}] = 50 \mu\text{M}$). Linear initial rates indicated that product inhibition was not problematic under the assay conditions. Inhibitors 1 and 3 were shown to bind with IC_{50} values of $32 \pm 4 \mu\text{M}$ and $1.5 \pm 1 \mu\text{M}$, respectively (Table 1, Figure 8). This mirrors the scenario with dehydrosqualene synthase, in which the uncharged inhibitor is more potent, and indicates that the positively charged guanidinium functionality is not essential for binding.

Table 1. Summary of Kinetic Constants Measured with DSQS and SQS

	K_{i} for DSQS (μM)	IC_{50} for SQS (μM) ^{a,b}	IC_{50} for DSQS (μM) ^a
inhibitor 1	1.9 ± 0.2	32 ± 4	17 ± 1
inhibitor 2	4.2 ± 0.7	212 ± 7	45 ± 2
inhibitor 3	0.6 ± 0.1	1.5 ± 1	5.5 ± 0.2

^aMeasured with $[\text{FPP}] = 50 \mu\text{M}$. ^bMeasured for the first half reaction in the absence of NADPH

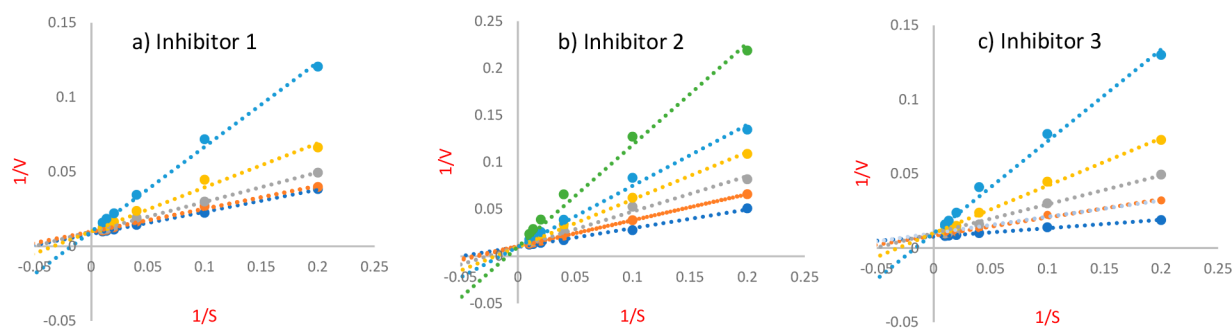


Figure 7. Lineweaver–Burk plots for the inhibition of dehydroqualene synthase by inhibitors 1–3. (A) Inhibition by inhibitor 1 at the following concentrations: light blue = 8.25 μM , yellow = 3.3 μM , gray = 1.6 μM , orange = 0.8 μM , dark blue = 0 μM . (B) Inhibition by inhibitor 2 at the following concentrations: green = 36 μM , light blue = 18 μM , yellow = 12 μM , gray = 9 μM , orange = 4.5 μM , dark blue = 0 μM . Inhibition by inhibitor 3 at the following concentrations: light blue = 8.25 μM , yellow = 3.3 μM , gray = 1.6 μM , orange = 0.8 μM , dark blue = 0 μM .

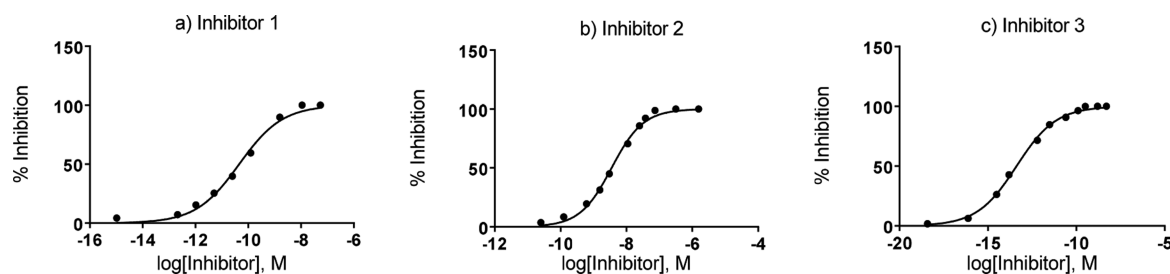


Figure 8. IC_{50} plots for the inhibition of the first half reaction of human squalene synthase by inhibitors 1–3. In each case, the concentration of FPP is 50 μM .

Surprisingly, inhibitor 2 was a somewhat weaker inhibitor of squalene synthase, showing an IC_{50} value of $212 \pm 7 \mu\text{M}$. The corresponding IC_{50} values of inhibitors 1, 2, and 3 determined for dehydroqualene synthase under identical FPP concentrations are 17, 45, and 5.5 μM , respectively (Table 1, Figure S3). While a comparison of the magnitudes of IC_{50} values between the DSQS full reaction and the “crippled” SQS half reaction are perhaps not justified, it should be noted that the trends are similar, with the uncharged inhibitor binding the tightest. Since the SQS half reaction is presumed to involve the formation of a carbocation intermediate using a similar mechanism to that of either the full SQS reaction or the DSQS reaction, the notion that this enzyme binds tightly to the carbocation intermediate is brought into question.

DISCUSSION

This study was initiated to probe the effectiveness of incorporating a guanidinium or amidinium group into inhibitors of squalene or dehydroqualene synthase. The functional groups introduce a planar, delocalized, cation in a position analogous to that of the putative allylic carbocation in the active site of the enzyme. It was anticipated that the enzymes would bind tightly to such species as they presumably have evolved to stabilize carbocationic intermediates and the transition states leading to them. Inhibitors 1 and 2 were found to inhibit dehydroqualene synthase with a low micromolar affinity, which is about 1 order of magnitude lower than the value of K_M for FPP. Both squalene and dehydroqualene synthases possess two distinct FPP-binding sites, only one which promotes ionization in the first step of the mechanism. It is not known which FPP-binding site the inhibitors occupy (perhaps even both); however, the kinetics showed competitive inhibition, and one would presume that the positively charged inhibitor would prefer to occupy the site of initial

ionization. Surprisingly, the urea-containing inhibitor 3 bound slightly more tightly than inhibitors 1 or 2 despite its lacking a positive charge. Similar trends were observed with these inhibitors in the first half reaction catalyzed by squalene synthase.

Several scenarios can account for the failure of the cationic functional groups to increase the potency of the inhibitors. One possibility is that the enzyme does not make specific binding interactions with the allylic carbocation during catalysis. As this mechanism requires several rearrangements and there are multiple spatially distinct positions that a carbocation must occupy during catalysis, it may not be necessary for nature to evolve an active site that is able to stabilize all of them. Instead, the initial dissociation of FPP may be induced by tight binding to the pyrophosphate as well as to the hydrophobic tail. A cluster of three Mg^{2+} ions interacts strongly with the pyrophosphate leaving group, and a long hydrophobic tunnel binds the FPP hydrophobic region.^{18,48} If these binding interactions are optimized in the transition state for the initial dissociation event, it may not be necessary for the enzyme to directly stabilize the carbocation via electrostatic interactions. This conversion of binding energy into catalytic efficiency is reminiscent of the Circe effect described by Jencks.⁴⁹ As the metal-coordinated pyrophosphate is a good leaving group, and the carbocation is tertiary, resonance stabilized, and bears no destabilizing electronegative atoms, it is reasonable to suspect that substrate binding interactions would suffice to promote ionization. Furthermore, the initially formed allylic carbocation will be stabilized by electrostatic interactions with the pyrophosphate of the ion pair. In a similar vein, the concept that terpene synthases are not directly involved in promoting many of the carbocation rearrangement/cyclization steps of catalysis has been forwarded in the literature.⁵⁰

A second possibility is that an allylic carbocation is never formed during catalysis. As direct evidence for such a species is lacking,²⁴ it is conceivable that the cyclopropanation reaction that forms presqualene diphosphate could occur in a single concerted step without a discrete carbocation intermediate. This seems somewhat unlikely given the precedence for carbocation intermediates in reactions of enzymes that utilize allylic diphosphates as substrates, and even if this were the case, one would expect the transition state for cyclopropanation to bear a considerable cationic character. Thus, one would still expect the positively charged inhibitors to bind more tightly than those lacking the positive charge.

A third scenario is that the guanidinium/amidinium cations are miss-positioned in the active site and do not pick up the binding interactions that normally are responsible for catalysis. While it is difficult to disprove this possibility, an examination of other attempts to inhibit squalene synthase with ammonium-containing FPP analogues suggests that this may not be the case. In one of the first reports of a potent squalene synthase inhibitor, a farnesyl tail was attached to the same phosphonylphosphinate moiety described in these studies by a variety of two atom linkers (Figure 9).⁵¹ Inhibitor 17 bore a

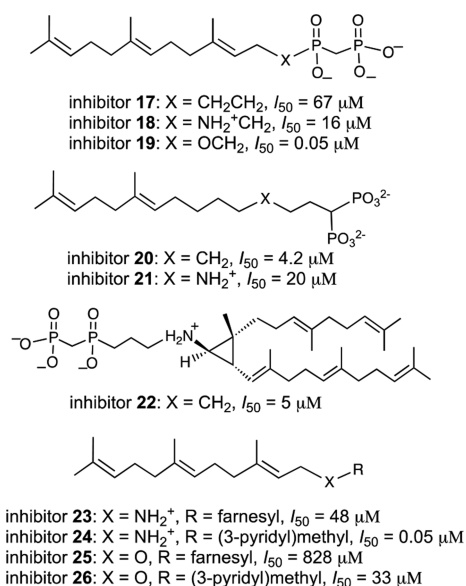


Figure 9. Selected squalene synthase inhibitors from the literature and their reported inhibition values.

two-carbon linker and inhibited the enzyme with an IC₅₀ of 67 μM. When one methylene was replaced with an ammonium functionality in inhibitor 18, the potency was only reduced 5-fold to give an IC₅₀ of 16 μM. This value is similar to that observed with the guanidinium/amidinium inhibitors 1 and 2 described in this study. Finally, when one of the methylene groups was replaced by an oxygen atom to give inhibitor 19, an IC₅₀ of 0.05 μM was measured. The greatly increased potency of this inhibitor was attributed to a putative hydrogen bond between the enzyme and the oxygen atom of the linker that would not exist in the other two compounds. Nevertheless, this work further demonstrates the minimal advantage of introducing a positive charge into the inhibitor design. An additional example can be found in studies with lipophilic 1,1-bisphosphonates, which are known potent inhibitors of many allylic pyrophosphate-utilizing enzymes.⁵² A bisphosphonate

bearing a purely hydrocarbon tail, inhibitor 20, displayed an IC₅₀ value of 4.2 nM against squalene synthase. When an ammonium functionality was introduced into the C-4 position to give inhibitor 21, the IC₅₀ value actually increased to 20 nM. Given the work described in this study and the literature reports presented above, there is little evidence that positively charged FPP analogues provide substantial additional binding in dSQS and SQS inhibitors. This provides indirect support to the notion that these enzymes do not directly stabilize the allylic carbocations during catalysis.

Finally, it is possible that these inhibitors only bind to the “nonionizing FPP site” and either have no affinity for the “ionization site” or bind to it in a manner that prevents the enzyme from adopting a conformation required for carbocation formation. In these scenarios, the guanidinium/amidinium functionalities would never be placed in an intact carbocation-stabilizing pocket and the advantages of the positive charge would not be realized. While one might expect that the structural similarity between the inhibitors and FPP would allow them to access either binding site, it is possible that the phosphonylphosphinate functionality is not accommodated by the cluster of divalent metal ions in the “ionization site”. This scenario would have to hold not only for inhibitors 1–3 but also for inhibitors 17–19 and 20–21 that likewise do not realize the potential benefit of the ammonium functionalities (Figure 9).

The case for the use of cationic inhibitors in the inhibition of the second half of the squalene synthase reaction is somewhat stronger. Poulter and co-workers targeted the second half of the squalene synthase reaction, which involves the ionization of presqualene diphosphate. Inhibitor 22 is a mimic of presqualene diphosphate, in which an ammonium functionality has been placed in the position where a cyclopropylmethyl cation would be expected to form.⁵³ This inhibitor was found to inhibit squalene synthase with an IC₅₀ of 5 μM, which compares favorably to the reported *K*_M value of 77 μM for the reaction of presqualene diphosphate in the second half of the SQS reaction.²⁴ In another report, a series of aziridine analogues of presqualene pyrophosphate was found to inhibit the enzyme with IC₅₀ values in the range of 1–10 μM.⁵⁴ In both of these studies, isosteric analogues lacking the positive charge were unavailable for comparison. A convincing report on the importance of a positive charge toward binding of squalene synthase inhibitors showed that secondary amines such as 23 and 24 bound as much as 3 orders of magnitude more tightly than their corresponding ether analogues, 25 and 26. This was interpreted as being due to the protonated amines acting as analogues of carbocation intermediates involved in the conversion of presqualene diphosphate to squalene.⁵⁵ Finally, some very potent inhibitors that bear protonatable amines have been uncovered in drug discovery efforts, and it has been postulated that these positive charges are acting as mimics of carbocationic intermediates.^{13,56}

The use of protonated amines as mimics of carbocation intermediates and/or transition states has been an effective tool for developing potent inhibitors against many families of enzymes. In particular, this strategy is effective in the inhibition of glycosidases,^{14,15,57} and nucleoside phosphorylases/hydrolases.¹⁶ Inhibitors that utilize a protonated amine as an oxocarbenium ion mimic have been shown to serve as potent inhibitors with *K*_i values in the nanomolar to picomolar range. The tight binding of these inhibitors is a result of the enzyme’s affinity for a transition state/intermediate, in which a

significant positive charge is developed. When one compares the reaction of glycosidases to that of enzymes that promote the dissociation of allylic diphosphates, key differences emerge. Most importantly, in glycosidases, the leaving group (typically an alcohol) is a much poorer leaving group than pyrophosphate and has less ability to be assisted by charged hydrogen bonds or metal ion catalysis. Additionally, the oxocarbenium ion is arguably less stable than a tertiary allylic carbocation, particularly as sugars are heavily substituted by electron-withdrawing oxygen atoms.^{58–62} For these reasons, one would expect that the glycosidase would necessarily have to evolve to stabilize the oxocarbenium ion (or oxocarbenium-like transition state) in order to promote its formation.

Ammonium-containing inhibitors have also been quite effective with enzymes that generate tertiary carbocations from the protonation or alkylation of alkenes.^{63–65} Several differences exist between these reactions and those involving the dissociation allylic of allylic diphosphates. First, a tertiary carbocation is much higher in energy than an allylic tertiary carbocation as it is not resonance stabilized. Second, it is not possible to use tight binding to the diphosphate moiety to assist catalysis. Finally, there is no pyrophosphate present in the active site that acts as an ion pair and serves to stabilize the carbocation via electrostatic interactions. Thus, it seems reasonable to expect that these enzymes would also evolve to bind tightly to the carbocation as part of the catalytic strategy.

These studies suggest that the active sites of dehydrosqualene synthase and squalene synthase did not need to evolve a high affinity for the allylic carbocation formed from the dissociation of FPP. It is possible that this phenomenon is more general and can be found in other enzymes that promote the dissociation of allylic diphosphates, including prenyltransferases, terpene cyclases, and allylic diphosphate synthases. In particular, the terpene cyclases also form carbocationic species that may undergo multiple carbocation rearrangements within a single active site.²² Studies with ammonium- or sulfonium-based inhibitors of terpene cyclases have been reported, but they are often used as coinhibitors with high concentrations of free pyrophosphate.^{66–69} The K_i values obtained are often in the low micromolar range, which is not far from the value of K_M for the allylic diphosphate substrate. One clear example of where positively charged inhibitors do provide tight binding is in the case of the allylic diphosphate synthases (FPP synthase and geranylgeranyl diphosphate synthase).^{70–75} These enzymes are strongly inhibited by 1,1-bisphosphonates and, in particular, the nitrogen-containing bisphosphonates (see compound **21** in Figure 9 for an example). These compounds bear an amine located two or three carbons away from the bisphosphonate that is thought to provide the cationic charge that mimics the allylic carbocation. This amine may in the form of an ammonium, a pyridinium, an imidazolium, or a guanidinium and the presence of the amine serves to increase the affinity of the inhibitors by 1–2 orders of magnitude. In many cases, the K_i of these inhibitors is in the nanomolar range, far below the K_M of the substrate. An ammonium-containing inhibitor of protein farnesyltransferase has also been reported, and while the IC_{50} value was only 14 μM , the replacement of the amine with a sulfur atom increased the IC_{50} value to >200 μM . Therefore, the inhibition results with dehydrosqualene synthase cannot be generalized to all enzymes that catalyze the dissociation of an allylic diphosphate in the first step of catalysis. Instead this work suggests that a “carbocation mimic” approach to inhibitor design may be

effective with many members of the above-mentioned families, but not necessarily with all of them.

■ ASSOCIATED CONTENT

📄 Supporting Information

The Supporting Information is available free of charge on the ACS Publications website at DOI: 10.1021/acs.biochem.8b00731.

Michaelis–Menten plots, IC_{50} graphs, and NMR spectra for newly synthesized compounds (PDF)

■ AUTHOR INFORMATION

Corresponding Author

*E-mail: mtanner@chem.ubc.ca. Phone: (604) 822-9453.

ORCID

Martin E. Tanner: 0000-0002-3224-3491

Funding

This work was supported by a grant from the Natural Sciences and Engineering Council of Canada (NSERC) to M.E.T.

Notes

The authors declare no competing financial interest.

■ REFERENCES

- (1) Liang, P.-H., Ko, T.-P., and Wang, A. H.-J. (2002) Structure, mechanism and function of prenyltransferases. *Eur. J. Biochem.* 269, 3339–3354.
- (2) Kellogg, B. A., and Poulter, C. D. (1997) Chain elongation in the isoprenoid biosynthetic pathway. *Curr. Opin. Chem. Biol.* 1, 570–578.
- (3) Christianson, D. W. (2006) Structural biology and chemistry of the terpenoid cyclases. *Chem. Rev.* 106, 3412–3442.
- (4) Ochocki, J. D., and Distefano, M. D. (2013) Prenyltransferase inhibitors: Treating human ailments from cancer to parasitic infections. *MedChemComm* 4, 476–492.
- (5) Oldfield, E. (2010) Targeting isoprenoid biosynthesis for drug discovery: Bench to bedside. *Acc. Chem. Res.* 43, 1216–1226.
- (6) Poulter, C. D., Wiggins, P. L., and Le, A. T. (1981) Farnesylpyrophosphate synthetase. A stepwise mechanism for the 1'-4 condensation reaction. *J. Am. Chem. Soc.* 103, 3926–3927.
- (7) Mash, E. A., Gurria, G. M., and Poulter, C. D. (1981) Farnesylpyrophosphate synthetase. Evidence for a rigid geranyl cation-pyrophosphate anion pair. *J. Am. Chem. Soc.* 103, 3927–3929.
- (8) Luk, L. Y. P., and Tanner, M. E. (2009) Mechanism of dimethylallyltryptophan synthase: Evidence for a dimethylallyl cation intermediate in an aromatic prenyltransferase. *J. Am. Chem. Soc.* 131, 13932–13933.
- (9) Cane, D. E., and Iyengar, R. (1979) The enzymatic conversion of farnesyl to nerolidyl pyrophosphate: Role of the pyrophosphate moiety. *J. Am. Chem. Soc.* 101, 3385–3388.
- (10) Weller, V. A., and Distefano, M. D. (1998) Measurement of the α -secondary kinetic isotope effect for a prenyltransferase by MALDI mass spectrometry. *J. Am. Chem. Soc.* 120, 7975–7976.
- (11) Huang, C.-C., Hightower, K. E., and Fierke, C. A. (2000) Mechanistic studies of rat protein farnesyltransferase indicate an associative transition state. *Biochemistry* 39, 2593–2602.
- (12) Harris, C. M., and Poulter, C. D. (2000) Recent studies of the mechanism of protein prenylation. *Nat. Prod. Rep.* 17, 137–144.
- (13) Biller, S. A., Neuenschwander, K., Ponpipom, M. M., and Poulter, C. D. (1996) Squalene synthase inhibitors. *Curr. Pharm. Design* 2, 1–40.
- (14) Gloster, T. M., and Davies, G. J. (2010) Glycosidase inhibition: Assessing mimicry of the transition state. *Org. Biomol. Chem.* 8, 305–320.
- (15) Liu, Z. Y., and Ma, S. T. (2017) Recent advances in synthetic glucosidase inhibitors. *ChemMedChem* 12, 819–829.

- (16) Schramm, V. L. (2013) Transition states, analogues, and drug development. *ACS Chem. Biol.* 8, 71–81.
- (17) Poulter, C. D. (1990) Biosynthesis of Non-Head-to-Tail Terpenes - Formation of 1'-1 and 1'-3 Linkages. *Acc. Chem. Res.* 23, 70–77.
- (18) Lin, F. Y., Liu, C. I., Liu, Y. L., Zhang, Y. H., Wang, K., Jeng, W. Y., Ko, T. P., Cao, R., Wang, A. H. J., and Oldfield, E. (2010) Mechanism of action and inhibition of dehydroqualene synthase. *Proc. Natl. Acad. Sci. U. S. A.* 107, 21337–21342.
- (19) Gu, P. D., Ishii, Y., Spencer, T. A., and Shechter, I. (1998) Function-structure studies and identification of three enzyme domains involved in the catalytic activity in rat hepatic squalene synthase. *J. Biol. Chem.* 273, 12515–12525.
- (20) Blagg, B. S. J., Jarstfer, M. B., Rogers, D. H., and Poulter, C. D. (2002) Recombinant squalene synthase. A mechanism for the rearrangement of presqualene diphosphate to squalene. *J. Am. Chem. Soc.* 124, 8846–8853.
- (21) Jarstfer, M. B., Blagg, B. S. J., Rogers, D. H., and Poulter, C. D. (1996) Biosynthesis of squalene. Evidence for a tertiary cyclopropylcarbinyl cationic intermediate in the rearrangement of presqualene diphosphate to squalene. *J. Am. Chem. Soc.* 118, 13089–13090.
- (22) Christianson, D. W. (2017) Structural and chemical biology of terpenoid cyclases. *Chem. Rev.* 117, 11570–11648.
- (23) Wieland, B., Feil, C., Gloriamercker, E., Thumm, G., Lechner, M., Bravo, J. M., Poralla, K., and Gotz, F. (1994) Genetic and biochemical analyses of the biosynthesis of the yellow carotenoid 4,4'-diaponeurosporene of *Staphylococcus Aureus*. *J. Bacteriol.* 176, 7719–7726.
- (24) Radisky, E. S., and Poulter, C. D. (2000) Squalene synthase: Steady-state, pre-steady-state, and isotope-trapping studies. *Biochemistry* 39, 1748–1760.
- (25) Kourounakis, A. P., Katselou, M. G., Matralis, A. N., Ladopoulou, E. M., and Bavavea, E. (2011) Squalene synthase inhibitors: An update on the search for new antihyperlipidemic and antiatherosclerotic Agents. *Curr. Med. Chem.* 18, 4418–4439.
- (26) Nadin, A., and Nicolaou, K. C. (1996) Chemistry and biology of the zaragozic acids (squalostatins). *Angew. Chem., Int. Ed. Engl.* 35, 1622–1656.
- (27) Stein, E. A., Bays, H., O'Brien, D., Pedicano, J., Piper, E., and Spezzi, A. (2011) Lapaquistat acetate development of a squalene synthase inhibitor for the treatment of hypercholesterolemia. *Circulation* 123, 1974–1985.
- (28) Liu, C. I., Liu, G. Y., Song, Y. C., Yin, F. L., Hensler, M. E., Jeng, W. Y., Nizet, V., Wang, A. H. J., and Oldfield, E. (2008) A cholesterol biosynthesis inhibitor blocks *Staphylococcus aureus* virulence. *Science* 319, 1391–1394.
- (29) Liu, G. Y., and Nizet, V. (2009) Color me bad: microbial pigments as virulence factors. *Trends Microbiol.* 17, 406–413.
- (30) Bradford, M. M. (1976) A rapid and sensitive method for the quantitation of microgram quantities of protein utilizing the principle of protein-dye binding. *Anal. Biochem.* 72, 248–254.
- (31) Inoue, H., Nojima, H., and Okayama, H. (1990) High-efficiency transformation of *Escherichia coli* with plasmids. *Gene* 96, 23–28.
- (32) Song, Y. C., Lin, F. Y., Yin, F. L., Hensler, M., Poveda, C. A. R., Mukkamala, D., Cao, R., Wang, H., Morita, C. T., Pacanowska, D. G., Nizet, V., and Oldfield, E. (2009) Phosphonosulfonates are potent, selective inhibitors of dehydroqualene synthase and staphyloxanthin biosynthesis in *Staphylococcus aureus*. *J. Med. Chem.* 52, 976–988.
- (33) Webb, M. R. (1992) A continuous spectrophotometric assay for inorganic phosphate and for measuring phosphate release kinetics in biological systems. *Proc. Natl. Acad. Sci. U. S. A.* 89, 4884–4887.
- (34) Mori, K., and Funaki, Y. (1985) Synthesis of sphingosine relatives. 2. Synthesis of (4E,8E,2S,3R,2'R)-N-2'-hydroxyhexadecanoyl-9-methyl-4,8-sphingadienine, the ceramide portion of the fruiting-inducing cerebroside in a Basidiomycete *Schizophyllum commune*, and its (2R,3S)-isomer. *Tetrahedron* 41, 2369–2377.
- (35) Nacs, E. D., and Lambert, T. H. (2015) Higher-order cyclopropenimine superbases: Direct neutral Bronsted base catalyzed Michael reactions with α -aryl esters. *J. Am. Chem. Soc.* 137, 10246–10253.
- (36) Flohr, A., Aemissegger, A., and Hilvert, D. (1999) α -Functionalized phosphonylphosphinates: Synthesis and evaluation as transcarbamoylase inhibitors. *J. Med. Chem.* 42, 2633–2640.
- (37) Yin, B. L., Liu, Z. G., Zhang, J. C., and Li, Z. R. (2010) N,N'-Di-Boc-substituted thiourea as a novel and mild thioacylating agent applicable for the synthesis of thiocarbonyl compounds. *Synthesis* 2010, 991–999.
- (38) Linton, B. R., Carr, A. J., Orner, B. P., and Hamilton, A. D. (2000) A versatile one-pot synthesis of 1,3-substituted guanidines from carbamoyl isothiocyanates. *J. Org. Chem.* 65, 1566–1568.
- (39) Diaz, D. D., and Finn, M. G. (2004) Modular synthesis of formamidines and their formation of stable organogels. *Chem. Commun.*, 2514–2516.
- (40) Porcheddu, A., Giacomelli, G., and Piredda, I. (2009) Parallel synthesis of trisubstituted formamidines: A facile and versatile procedure. *J. Comb. Chem.* 11, 126–130.
- (41) Zhou, X., Reilly, J. E., Loerch, K. A., Hohl, R. J., and Wiemer, D. F. (2014) Synthesis of isoprenoid bisphosphonate ethers through C-P bond formations: Potential inhibitors of geranylgeranyl diphosphate synthase. *Beilstein J. Org. Chem.* 10, 1645–1650.
- (42) Spyropoulos, C., and Kokotos, C. G. (2014) One-pot synthesis of ureas from Boc-protected amines. *J. Org. Chem.* 79, 4477–4483.
- (43) Thompson, J. F., Danley, D. E., Mazzalupo, S., Milos, P. M., Lira, M. E., and Harwood, H. J. (1998) Truncation of human squalene synthase yields active, crystallizable protein. *Arch. Biochem. Biophys.* 350, 283–290.
- (44) Milner-White, E. J. (1997) The partial charge of the nitrogen atom in peptide bonds. *Protein Sci.* 6, 2477–2482.
- (45) Beytia, E., Qureshi, A. A., and Porter, J. W. (1973) Squalene synthetase. 3. Mechanism of reaction. *J. Biol. Chem.* 248, 1856–1867.
- (46) Soltis, D. A., McMahon, G., Caplan, S. L., Dudas, D. A., Chamberlin, H. A., Vattay, A., Dottavio, D., Rucker, M. L., Engstrom, R. G., Cornellkennon, S. A., and Boettcher, B. R. (1995) Expression, purification, and characterization of the human squalene synthase - Use of yeast and baculoviral systems. *Arch. Biochem. Biophys.* 316, 713–723.
- (47) Zhang, D. L., and Poulter, C. D. (1995) Biosynthesis of non-head-to-tail isoprenoids - Synthesis of 1'-1-structures and 1'-3-structures by recombinant yeast squalene synthase. *J. Am. Chem. Soc.* 117, 1641–1642.
- (48) Pandit, J., Danley, D. E., Schulte, G. K., Mazzalupo, S., Pauly, T. A., Hayward, C. M., Hamanaka, E. S., Thompson, J. F., and Harwood, H. J. (2000) Crystal structure of human squalene synthase - A key enzyme in cholesterol biosynthesis. *J. Biol. Chem.* 275, 30610–30617.
- (49) Jencks, W. P. (2006) Binding-energy, specificity, and enzymic catalysis - Circe effect. *Adv. Enzymol. Relat. Areas Mol. Biol.* 43, 219–410.
- (50) Tantilillo, D. J. (2017) Importance of inherent substrate reactivity in enzyme-promoted carbocation cyclization/rearrangements. *Angew. Chem., Int. Ed.* 56, 10040–10045.
- (51) Biller, S. A., Sofia, M. J., Delange, B., Forster, C., Gordon, E. M., Harrity, T., Rich, L. C., and Ciosek, C. P. (1991) The 1st potent inhibitor of squalene synthase - A profound contribution of an ether oxygen to inhibitor enzyme interaction. *J. Am. Chem. Soc.* 113, 8522–8524.
- (52) Ciosek, C. P., Magnin, D. R., Harrity, T. W., Logan, J. V. H., Dickson, J. K., Gordon, E. M., Hamilton, K. A., Jolibois, K. G., Kunselman, L. K., Lawrence, R. M., Mookhtiar, K. A., Rich, L. C., Slusarchyk, D. A., Sulsky, R. B., and Biller, S. A. (1993) Lipophilic 1,1-bisphosphonates Are potent squalene synthase inhibitors and orally-active cholesterol-lowering agents in-vivo. *J. Biol. Chem.* 268, 24832–24837.
- (53) Poulter, C. D., Capson, T. L., Thompson, M. D., and Bard, R. S. (1989) Squalene synthetase - Inhibition by ammonium analogs of

carbocationic intermediates in the conversion of presqualene diphosphate to squalene. *J. Am. Chem. Soc.* 111, 3734–3739.

(54) Koohang, A., Bailey, J. L., Coates, R. M., Erickson, H. K., Owen, D., and Poulter, C. D. (2010) Enantioselective inhibition of squalene synthase by aziridine analogues of presqualene diphosphate. *J. Org. Chem.* 75, 4769–4777.

(55) Prashad, M., Kathawala, F. G., and Scallen, T. (1993) *N*-(Arylalkyl)farnesylamines - New potent squalene synthetase inhibitors. *J. Med. Chem.* 36, 1501–1504.

(56) Sealey-Cardona, M., Cammerer, S., Jones, S., Ruiz-Perez, L. M., Brun, R., Gilbert, I. H., Urbina, J. A., and Gonzalez-Pacanowska, D. (2007) Kinetic characterization of squalene synthase from *Trypanosoma cruzi*: Selective inhibition by quinuclidine derivatives. *Antimicrob. Agents Chemother.* 51, 2123–2129.

(57) Asano, N. (2003) Glycosidase inhibitors: update and perspectives on practical use. *Glycobiology* 13, 93R–104R.

(58) Martin, A., Arda, A., Desire, J., Martin-Mingot, A., Probst, N., Sinay, P., Jimenez-Barbero, J., Thibaudeau, S., and Bleriot, Y. (2016) Catching elusive glycosyl cations in a condensed phase with HF/SbF₅ superacid. *Nat. Chem.* 8, 186–191.

(59) Olah, G. A., Clifford, P. R., Halpern, Y., and Johanson, R. G. (1971) Stable carbocations. CXIX. Carbon-13 nuclear magnetic resonance spectroscopy study of the structure of allyl cations. *J. Am. Chem. Soc.* 93, 4219–4222.

(60) Amyes, T. L., and Jencks, W. P. (1989) Lifetimes of oxocarbenium ions in aqueous solution from common ion inhibition of the solvolysis of α -azido ethers by added azide ion. *J. Am. Chem. Soc.* 111, 7888–7900.

(61) Richard, J. P., Amyes, T. L., and Toteva, M. M. (2001) Formation and stability of carbocations and carbanions in water and intrinsic barriers to their reactions. *Acc. Chem. Res.* 34, 981–988.

(62) Rablen, P. R., and Perry-Freer, N. A. (2018) How the arrangement of alkyl substituents affects the stability of delocalized carbocations. *J. Org. Chem.* 83, 4024–4033.

(63) Muehlbacher, M., and Poulter, C. D. (1985) Isopentenyl diphosphate:dimethylallyl diphosphate isomerase. Irreversible inhibition of the enzyme by active-site directed covalent attachment. *J. Am. Chem. Soc.* 107, 8307–8308.

(64) Narula, A. S., Rahier, A., Benveniste, P., and Schuber, F. (1981) 24-Methyl-25-azacycloartanol, an analog of a carbonium-ion high-energy intermediate, is a potent inhibitor of (*S*)-adenosyl-L-methionine - sterol C-24-methyltransferase in higher-plant cells. *J. Am. Chem. Soc.* 103, 2408–2409.

(65) Reardon, J. E., and Abeles, R. H. (1985) Time-dependent inhibition of isopentenyl pyrophosphate isomerase by 2-(dimethylamino)ethylpyrophosphate. *J. Am. Chem. Soc.* 107, 4078–4079.

(66) Cane, D. E., Yang, G. H., Coates, R. M., Pyun, H. J., and Hohn, T. M. (1992) Trichodiene synthase - Synergistic inhibition by inorganic pyrophosphate and aza analogs of the bisabolyl cation. *J. Org. Chem.* 57, 3454–3462.

(67) Croteau, R., Wheeler, C. J., Aksela, R., and Oehlschlager, A. C. (1986) Inhibition of monoterpene cyclases by sulfonium analogs of presumptive carbocationic intermediates of the cyclization reaction. *J. Biol. Chem.* 261, 7257–7263.

(68) Faraldos, J. A., and Allemann, R. K. (2011) Inhibition of (+)-aristolochene synthase with iminium salts resembling eudesmane cation. *Org. Lett.* 13, 1202–1205.

(69) Faraldos, J. A., Kariuki, B., and Allemann, R. K. (2010) Intermediacy of eudesmane cation during catalysis by aristolochene synthase. *J. Org. Chem.* 75, 1119–1125.

(70) Bergstrom, J. D., Bostedor, R. G., Masarachia, P. J., Reszka, A. A., and Rodan, G. (2000) Alendronate is a specific, nanomolar inhibitor of farnesyl diphosphate synthase. *Arch. Biochem. Biophys.* 373, 231–241.

(71) Hosfield, D. J., Zhang, Y. M., Dougan, D. R., Broun, A., Tari, L. W., Swanson, R. V., and Finn, J. (2004) Structural basis for bisphosphonate-mediated inhibition of isoprenoid biosynthesis. *J. Biol. Chem.* 279, 8526–8529.

(72) Martin, M. B., Arnold, W., Heath, H. T., III, Urbina, J. A., and Oldfield, E. (1999) Nitrogen-containing bisphosphonates as carbocation transition state analogs for isoprenoid biosynthesis. *Biochem. Biophys. Res. Commun.* 263, 754–758.

(73) No, J.-H., Dossin, F. D., Zhang, Y., Liu, Y.-L., Zhu, W., Feng, X., Yoo, J. A., Lee, E., Wang, K., Hui, R., Freitas-Junior, L. H., and Oldfield, E. (2012) Lipophilic analogs of zolendronate and risedronate inhibit *Plasmodium* geranylgeranyl diphosphate synthase (GGPPS) and exhibit potent antimalarial activity. *Proc. Natl. Acad. Sci. U. S. A.* 109, 4058–4063.

(74) Sanders, J. M., Gomez, A. O., Mao, J. H., Meints, G. A., Van Brussel, E. M., Burzynska, A., Kafarski, P., Gonzalez-Pacanowska, D., and Oldfield, E. (2003) 3-D QSAR investigations of the inhibition of Leishmania major farnesyl pyrophosphate synthase by bisphosphonates. *J. Med. Chem.* 46, 5171–5183.

(75) Zhang, Y., Cao, R., Yin, F., Hudock, M. P., Guo, R.-T., Krysiak, K., Mukherjee, S., Gao, Y.-G., Robinson, H., Song, Y., No, J.-H., Bergan, K., Leon, A., Cass, L., Goddard, A., Chang, T.-K., Lin, F. Y., Van Beek, E., Papapoulos, S., Wang, A. H.-J., Kubo, T., Ochi, M., Mukkamala, D., and Oldfield, E. (2009) Lipophilic bisphosphonates as dual farnesyl/geranylgeranyl diphosphate synthase inhibitors: an X-ray and NMR investigation. *J. Am. Chem. Soc.* 131, 5153–5162.